

Palaeoecological data indicates land-use changes across Europe linked to spatial heterogeneity in mortality during the Black Death pandemic

Article

Published Version

Creative Commons: Attribution 4.0 (CC-BY)

Open access

Izdebski, A. ORCID: <https://orcid.org/0000-0002-3456-5478>,
Guzowski, P. ORCID: <https://orcid.org/0000-0002-6494-4217>,
Poniat, R., Masci, L. ORCID: <https://orcid.org/0000-0003-1829-8418>, Palli, J., Vignola, C., Bauch, M., Coccozza, C.
ORCID: <https://orcid.org/0000-0002-8614-5459>, Fernandes,
R., Ljungqvist, F. C. ORCID: <https://orcid.org/0000-0003-0220-3947>,
Newfield, T. ORCID: <https://orcid.org/0000-0003-1451-5024>,
Seim, A., Abel-Schaad, D. ORCID: <https://orcid.org/0000-0003-3915-8342>,
Alba-Sánchez, F. ORCID: <https://orcid.org/0000-0003-0387-1533>,
Björkman, L., Brauer, A., Brown, A., Czerwiński, S. ORCID: <https://orcid.org/0000-0003-3422-040X>,
Ejarque, A. ORCID: <https://orcid.org/0000-0001-9101-5299>,
Fiłoc, M. ORCID: <https://orcid.org/0000-0003-1226-2676>,
Florenzano, A. ORCID: <https://orcid.org/0000-0003-4759-6406>,
Fredh, E. D. ORCID: <https://orcid.org/0000-0003-1787-6976>,
Fyfe, R., Jasiunas, N., Kołaczek, P., Kouli, K. ORCID: <https://orcid.org/0000-0003-1656-1091>,
Kozáková, R., Kupryjanowicz, M., Lagerås, P. ORCID: <https://orcid.org/0000-0002-2804-8028>,
Lamentowicz, M. ORCID: <https://orcid.org/0000-0003-0429-1530>,
Lindbladh, M., López-

Sáez, J. A., Luelmo-Lautenschlaeger, R. ORCID:
<https://orcid.org/0000-0002-4505-2416>, Marcisz, K. ORCID:
<https://orcid.org/0000-0003-2655-9729>, Mazier, F. ORCID:
<https://orcid.org/0000-0003-2643-0925>, Mensing, S., Mercuri,
A. M. ORCID: <https://orcid.org/0000-0001-6138-4165>, Milecka,
K., Miras, Y. ORCID: <https://orcid.org/0000-0002-4055-4134>,
Noryśkiewicz, A. M. ORCID: <https://orcid.org/0000-0002-9481-8684>,
Novenko, E., Obremaska, M. ORCID:
<https://orcid.org/0000-0002-3465-1894>, Panajiotidis, S.
ORCID: <https://orcid.org/0000-0003-1236-9000>,
Papadopoulou, M. L., Pędziszewska, A., Pérez-Díaz, S.
ORCID: <https://orcid.org/0000-0002-2702-0058>, Piovesan, G.
ORCID: <https://orcid.org/0000-0002-3214-0839>, Pluskowski, A.
ORCID: <https://orcid.org/0000-0002-4494-7664>, Pokorny, P.,
Poska, A., Reitalu, T. ORCID: <https://orcid.org/0000-0002-6555-3066>,
Rösch, M., Sadori, L. ORCID:
<https://orcid.org/0000-0002-2774-6705>, Sá Ferreira, C.,
Sebag, D. ORCID: <https://orcid.org/0000-0002-6446-6921>,
Słowiński, M. ORCID: <https://orcid.org/0000-0002-3011-2682>,
Stančikaitė, M. ORCID: <https://orcid.org/0000-0001-9425-5634>,
Stivrins, N., Tunno, I., Veski, S., Wacnik, A. ORCID:
<https://orcid.org/0000-0003-1104-0705> and Masi, A. ORCID:
<https://orcid.org/0000-0001-9822-9767> (2022)
Palaeoecological data indicates land-use changes across
Europe linked to spatial heterogeneity in mortality during the
Black Death pandemic. *Nature Ecology & Evolution*, 6. pp.
297-306. ISSN 2397-334X doi: <https://doi.org/10.1038/s41559-021-01652-4>
Available at
<https://centaur.reading.ac.uk/103311/>

It is advisable to refer to the publisher's version if you intend to cite from the work. See [Guidance on citing](#).

To link to this article DOI: <http://dx.doi.org/10.1038/s41559-021-01652-4>

Publisher: Nature

All outputs in CentAUR are protected by Intellectual Property Rights law, including copyright law. Copyright and IPR is retained by the creators or other copyright holders. Terms and conditions for use of this material are defined in the [End User Agreement](#).

www.reading.ac.uk/centaur

CentAUR

Central Archive at the University of Reading

Reading's research outputs online



OPEN

Palaeoecological data indicates land-use changes across Europe linked to spatial heterogeneity in mortality during the Black Death pandemic

A. Izdebski^{1,2}, P. Guzowski³, R. Poniat³, L. Masci^{4,5}, J. Palli^{6,7}, C. Vignola^{1,5}, M. Bauch⁸, C. Coccozza^{1,9}, R. Fernandes^{1,10,11}, F. C. Ljungqvist^{12,13,14}, T. Newfield^{15,16}, A. Seim^{17,18}, D. Abel-Schaad¹⁹, F. Alba-Sánchez¹⁹, L. Björkman²⁰, A. Brauer^{21,22}, A. Brown^{23,24}, S. Czerwiński²⁵, A. Ejarque^{26,27}, M. Fiłoc²⁸, A. Florenzano²⁹, E. D. Fredh³⁰, R. Fyfe³¹, N. Jasiunas³², P. Kołaczek²⁵, K. Kouli^{1,33}, R. Kozáková³⁴, M. Kupryjanowicz²⁸, P. Lagerås³⁵, M. Lamentowicz²⁵, M. Lindbladh³⁶, J. A. López-Sáez³⁷, R. Luelmo-Lautenschlaeger^{37,38}, K. Marcisz²⁵, F. Mazier³⁹, S. Mensing⁴⁰, A. M. Mercuri²⁹, K. Milecka⁴¹, Y. Miras⁴², A. M. Noryśkiewicz^{43,44}, E. Novenko^{45,46}, M. Obremaska⁴⁷, S. Panajiotidis⁴⁸, M. L. Papadopoulou⁴⁹, A. Pędziszewska⁵⁰, S. Pérez-Díaz⁵¹, G. Piovesan⁷, A. Pluskowski²⁴, P. Pokorny⁵², A. Poska^{53,54}, T. Reitalu^{53,55}, M. Rösch⁵⁶, L. Sadori⁵, C. Sá Ferreira⁵⁷, D. Sebag⁵⁸, M. Słowiński⁵⁹, M. Stančikaitė⁶⁰, N. Stivrins^{32,53,61}, I. Tunno⁶², S. Veski⁵³, A. Wacnik⁶³ and A. Masi^{1,5} ✉

The Black Death (1347–1352 CE) is the most renowned pandemic in human history, believed by many to have killed half of Europe's population. However, despite advances in ancient DNA research that conclusively identified the pandemic's causative agent (bacterium *Yersinia pestis*), our knowledge of the Black Death remains limited, based primarily on qualitative remarks in medieval written sources available for some areas of Western Europe. Here, we remedy this situation by applying a pioneering new approach, 'big data palaeoecology', which, starting from palynological data, evaluates the scale of the Black Death's mortality on a regional scale across Europe. We collected pollen data on landscape change from 261 radiocarbon-dated coring sites (lakes and wetlands) located across 19 modern-day European countries. We used two independent methods of analysis to evaluate whether the changes we see in the landscape at the time of the Black Death agree with the hypothesis that a large portion of the population, upwards of half, died within a few years in the 21 historical regions we studied. While we can confirm that the Black Death had a devastating impact in some regions, we found that it had negligible or no impact in others. These inter-regional differences in the Black Death's mortality across Europe demonstrate the significance of cultural, ecological, economic, societal and climatic factors that mediated the dissemination and impact of the disease. The complex interplay of these factors, along with the historical ecology of plague, should be a focus of future research on historical pandemics.

Few doubt that the mid-fourteenth-century Afro-Eurasian plague pandemic, the Black Death, killed tens of millions of people. In western Asia and Europe, where its spread and mortality are best understood, upwards of 50% of the population is thought to have died within approximately 5 years^{1–4}. Whole-genome sequencing confirms the pandemic as a novel introduction of the zoonotic bacterium *Yersinia pestis*^{5,6}. Yet, despite advances in palaeogenetics and generations of written-source-based research on the cultural and economic transformations plague is credited with accelerating, from the Renaissance to the 'Great Divergence'^{7,8}, much about the Black Death's spread and demographic impact remains poorly understood. The regionality of the plague's mortality is particularly underexplored, owing to the availability of written sources and the limits of traditional historical methods. Here we pioneer a new approach, big data palaeoecology (BDP), that leverages the field of palynology to evaluate the demographic impact of the Black Death on a regional scale across Europe, independent of written sources

and traditional archaeological material. Our analysis of 1,634 pollen samples from 261 sites, reflecting landscape change and agricultural activities, demonstrates Black Death mortality was far more spatially heterogeneous than previously recognized. Strikingly, BDP provides independent confirmation of the devastating toll of the Black Death reflected in written sources in some European regions, while establishing conclusively that the Black Death did not affect all regions equally. We attribute this mortality variation to cultural, ecological, economic, societal and climatic factors, which influenced *Y. pestis* dissemination and prevalence, generating regionally unique outcomes.

Estimating Black Death mortality

Multidisciplinary studies are redefining the Black Death. In recent years, palaeogeneticists have confirmed the pandemic's *Y. pestis* identity and established that the outbreak seeded novel plague reservoirs in Europe^{5,6}. Archaeologists and historians meanwhile have

A full list of affiliations appears at the end of the paper.

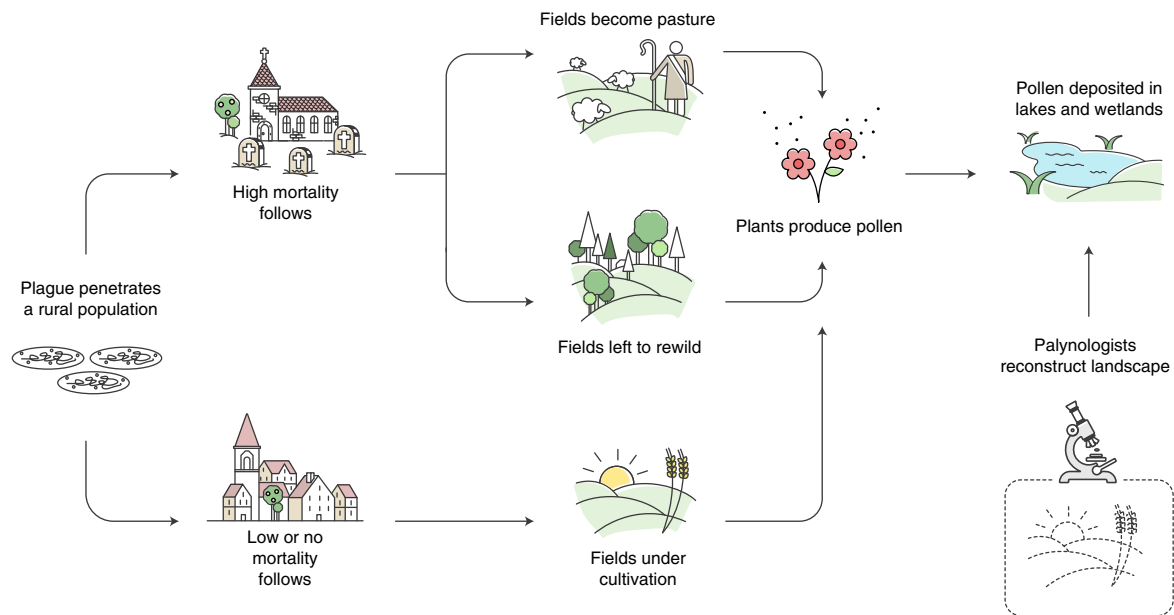


Fig. 1 | The BDP approach to verifying Black Death mortality levels. Credit: A.I., T.N., Hans Sell and Michelle O'Reilly.

begun to put sub-Saharan Africa on the Black Death map⁹, to fill in lacunae in our understanding of the pandemic's Mediterranean and European spread^{10,11}, and to explore the pandemic's origins in central Asia and dissemination in east Asia, drawing on evolutionary biology and palaeogenetics¹². But while multiple disciplines have reassessed the pandemic's spatiotemporality, its mortality—estimates of which have drawn attention to the Black Death for centuries—remains underexplored and limited almost entirely to unidisciplinary, written-source-based approaches.

Medieval mortality data are scarce and highly fragmentary. Nineteenth-century historians of the Black Death based their assertion that the pandemic claimed 25% or more of European lives on assessments of qualitative narrative sources¹³. Since the mid-twentieth century, historians have painstakingly built-up multiple instructive case studies of Black Death mortality for regions comparatively well-endowed with administrative sources allowing for statistical analysis (for example, regions of England, France, Italy and the Netherlands)^{14–16}. Some of these case studies have argued for a death toll in the range of 50% or more. These numbers have been increasingly considered representative of the Black Death's broader mortality^{1–4,9,12,14}. Although it has been suggested that regional variation characterized the demographic crisis the Black Death caused, little evidence—historical, archaeological or environmental—has been employed to substantiate such thinking^{8,17,18}. As a result, case studies from better documented regions have been employed as proxies for Black Death mortality in European regions where direct evidence for the pandemic is nonexistent (for example Bohemia and Finland), slight (single sentences or vague passages; for example Moravia, Hungary and Scotland) or available but neither detailed nor quantitative (most regions, including areas of England, France, Italy and the Netherlands)¹.

By treating case studies of relatively well-documented regions as predictive of the pandemic's death toll in all regions the pandemic touched, histories of the Black Death implicitly rest on the untested assumption that plague mortality was uniform across regions regardless of local cultural, ecological, economic and societal contexts, and therefore that the prevalence of *Y. pestis*, an ecologically and epidemiologically complex disease¹⁹, was comparable across Europe. This methodology has lent itself to estimates of an aggregate European death toll upwards of around 50% (approximately

50 million deaths)^{1,4}, though studies accounting for regional source scarcities have estimated mortality to have fallen below that mark^{8,17,20}. Problematically, many of the quantitative sources drawn upon to build case studies of Black Death mortality relate to urban contexts, which owing to their crowding, generally poor sanitation and quite possibly heavier disease burdens, may have suffered higher plague mortality than rural areas^{21,22}, and in the mid-fourteenth century upwards of 75–95% of the population of every European region was rural²³. Although every pandemic, plague or not, is distinct, a Black Death mortality across Europe of approximately 50% vastly exceeds the demographic losses sustained during the third plague pandemic in the late nineteenth century—the plague pandemic for which the most mortality data exists—including in China and India, which were then severely affected^{24,25}.

BDP and Black Death mortality

Here, we pioneer an alternative approach (discussed in detail in Methods). BDP allows us to evaluate the Black Death's mortality across Europe using quantitative palaeoenvironmental datasets, which can be employed for spatial statistical comparisons (Fig. 1). Our dataset consists of fossil pollen counts from 261 radiocarbon-dated sediment cores from 19 present-day European countries (Fig. 2; Supplementary Data 1). Pollen data can be used to assess past demographic dynamics as human pressure on the landscape in the pre-industrial period was directly dependent on the availability of rural labour. We focus on the period between 1250 and 1450 CE (comparing 100 years before and after the Black Death; 100 years representing roughly four generations, a time period during which pre-industrial populations could not recover from potentially high plague mortality²³) for which 1,634 pollen-analysed sediment samples are available (Supplementary Data 2).

In order to compare trends between different European bioclimatic zones, we assembled pollen types (taxa) representing different plants from species to family level into four standardized summary indicators, based on their subsistence value for human economy or their ecological needs as reflected in two major ecological indices, the Ellenberg light indicator and Niinemets and Valladares shade tolerance scale: (1) cereals; (2) herding (pasturelands); (3) fast forest secondary succession (pioneer shrubs and trees growing on former fields/pastures within 5–10 years of abandonment); (4) slow forest

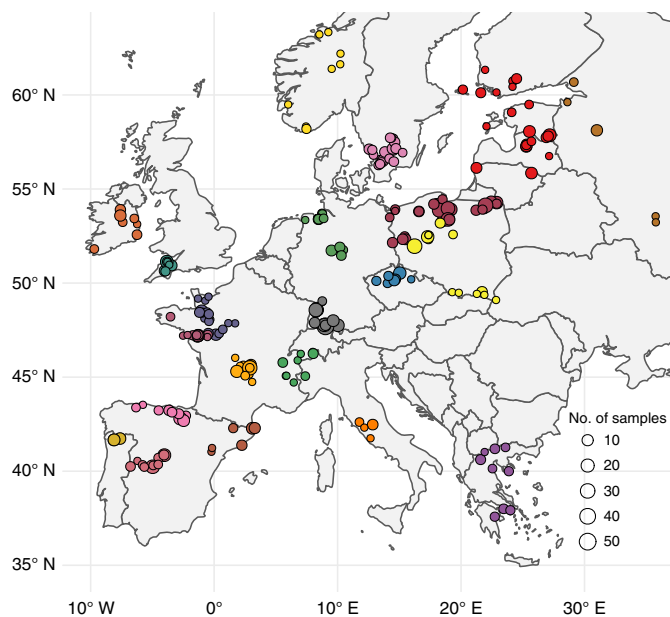


Fig. 2 | Location of pollen-analysed sediment cores used in this study. Circle size reflects the number of samples per site for the period of 1250–1450 CE, different colours reflect division of sites into regional clusters for the purpose of the analysis presented in Fig. 3.

secondary succession (mature–late successional woodland on abandoned fields/pastures). We discuss the results of the Ellenberg-based indicators below, but the Niinemets-based indicators yielded the same results in 19 out of 21 regions and the differences do not bear on our discussion (Extended Data Figs. 1 and 2).

Results

Validity test using Sweden and Poland. We validated our BDP approach by examining two well-studied, but contrasting, regional case studies of the Black Death's mortality, in Sweden and Poland. An earlier multidisciplinary analysis discovered significant contraction in cereal cultivation, as well as a more general economic and demographic decline, in the uplands of southern Sweden following the Black Death²⁶. By contrast, historians have long demonstrated that central Europe, particularly Poland, experienced economic growth over the fourteenth century, related to the centralization of royal power following a period of partition, few wars in the central provinces of the country, large-scale colonization of uncultivated lands and the development of cities²⁷. Our BDP approach independently corroborates these trajectories. We validate the ability of our pollen datasets to reflect the extent of the Black Death's mortality by comparing them to historical data of national tax payments made to the pope (Peter's pence)^{28–30} (Fig. 3). This validity test lends further support to our primary focus in this study on cereal cultivation, as argued in the Methods.

Four major scenarios of landscape and demographic change.

Having validated our approach, we analysed the pollen dataset for all of Europe. We focused on contrasting the four summary pollen indicator values on a regional scale for subperiods of 100 years before and after the Black Death. While we discuss the results of this analysis here (Fig. 4), our complimentary data presents 50-year (1301–1350 to 1351–1400) and 25-year (1325–1350 to 1351–1375) period analyses (Supplementary Figs. 1 and 2). For cereals, they returned the same results in terms of direction of change for 20 out of 21 regions for 50-year and 16 out of 19 regions for 25-year analyses, confirming the robustness of our conclusions (Extended

Data Fig. 3); the results for other indicators are also highly similar between different periods of analysis (Extended Data Figs. 4 and 5).

BDP employs bootstrapping to evaluate statistical significance of the differences between the pre- and post-Black Death subperiods on a regional level. In this way, we identified four scenarios of post-Black Death agricultural change based on the cereal pollen indicator (Fig. 4): (1) substantial and statistically significant increase, reflecting arable expansion and limited Black Death mortality (top panel); (2) modest and statistically insignificant increase, suggesting stability or slow-paced agrarian growth (upper middle panel); (3) modest and statistically insignificant decrease, suggesting stagnation or some contraction of agrarian activities, possibly stemming from more limited demographic losses or economic disruption caused by the plague (lower middle panel); (4) substantial and statistically significant decrease, reflecting arable contraction and pronounced Black Death mortality (bottom panel). Scenarios 1 and 2 falsify the theory that Black Death mortality was significant everywhere. Scenario 3 and 4 demonstrate Black Death mortality was devastating in some regions.

Changes in the herding indicator reveal trajectories similar to those of cereals in most cases or no change. We discovered only one region (southwest Germany) where there occurred a statistically significant decline in cultivation in parallel with a statistically significant increase in herding (some indication of this is also apparent in Greece), suggesting a shift to livestock production related to agrarian labour shortages and less demand for grain³¹. The fast forest succession indicator increases in a statistically significant way in central Italy and central France, confirming field abandonment. In central Italy, this is accompanied by discernible reforestation (statistically significant increase in the slow forest succession indicator), attesting to significant regional Black Death mortality and slow demographic and economic recovery.

To confirm the robustness of our results, BDP combines statistical with independent spatial approaches (Fig. 5). The latter yielded results identical for all four BDP indicators to our statistical approach in our 100-year period analysis as well as in our 50-year (1301–1350 CE to 1351–1400 CE) and 25-year (1325–1350 CE to 1351–1375 CE) period analyses (Supplementary Figs. 4–7).

Discussion

The Black Death was a diverse and entangled phenomenon.

Figure 6 visualizes the spatial distribution of the four trajectories of post-Black Death landscape change from Fig. 4, demonstrating that the Black Death's mortality varied significantly between European regions. The pandemic was immensely destructive in some areas, but in others it had a far lighter touch. Strikingly, BDP identifies a sharp agricultural decline in several regions of Europe, independently corroborating analyses of historical sources that suggest high mortality in regions of Scandinavia, France, western Germany, Greece and central Italy¹, and lending further validation to our approach. At the same time, there is much evidence for continuity and uninterrupted agricultural growth in central and eastern Europe, and several regions of western Europe, particularly in Ireland and Iberia. In this way, BDP invalidates histories of the Black Death that assume *Y. pestis* was uniformly prevalent, or nearly so, across Europe and that the pandemic had a devastating demographic impact everywhere.

While we have centred our study on estimating the impact of the Black Death on the landscape, plague recurred in several regions within the 100-, 50- and 25-year periods of our analyses. It is not implausible that some recurrences, notably the so-called *pestitis secunda* of the late 1350s and early 1360s³², could have been more devastating in a few regions we studied than the Black Death and that some of the arable contraction we detect may be attributable to both the Black Death and early second-pandemic recurrences. That the results of our 100-, 50- and 25-year period analyses were

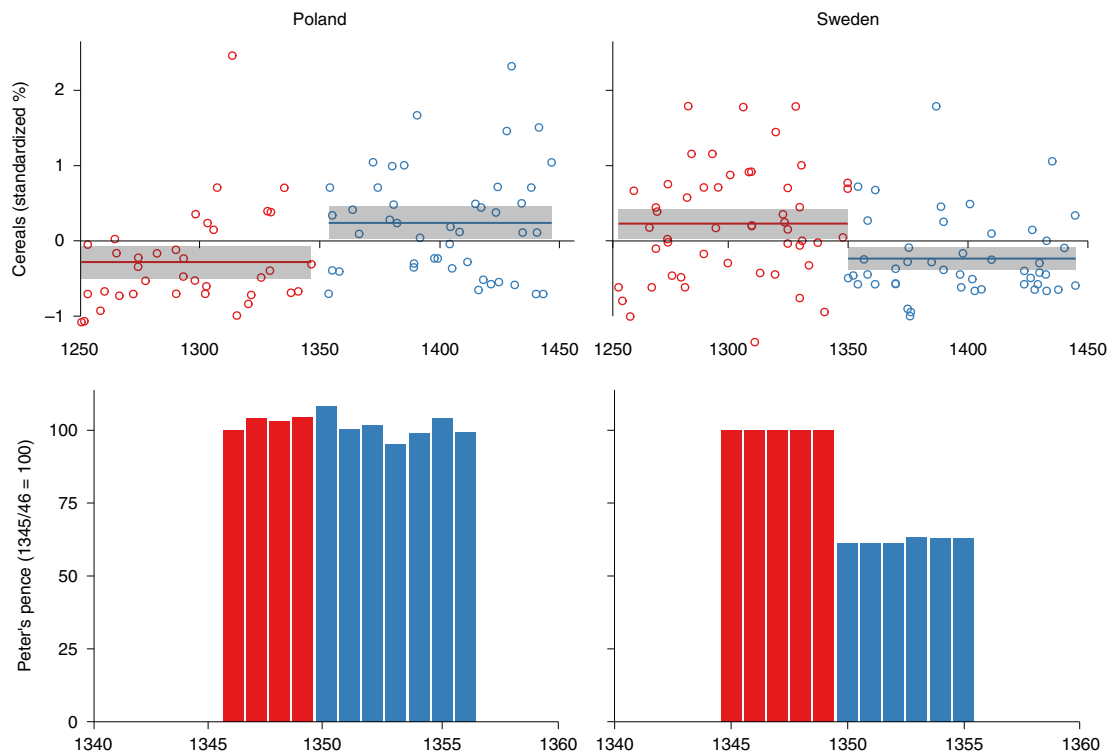


Fig. 3 | Comparison of historical and palaeoenvironmental indicators of the demographic impact of the Black Death in Poland and Sweden. Top panel, pollen data (cereal pollen, standardized percentage values from individual sites and 100-yr mean with standard deviation), see Supplementary Data 2. Bottom panel, Peter's pence tax²⁷⁻²⁹.

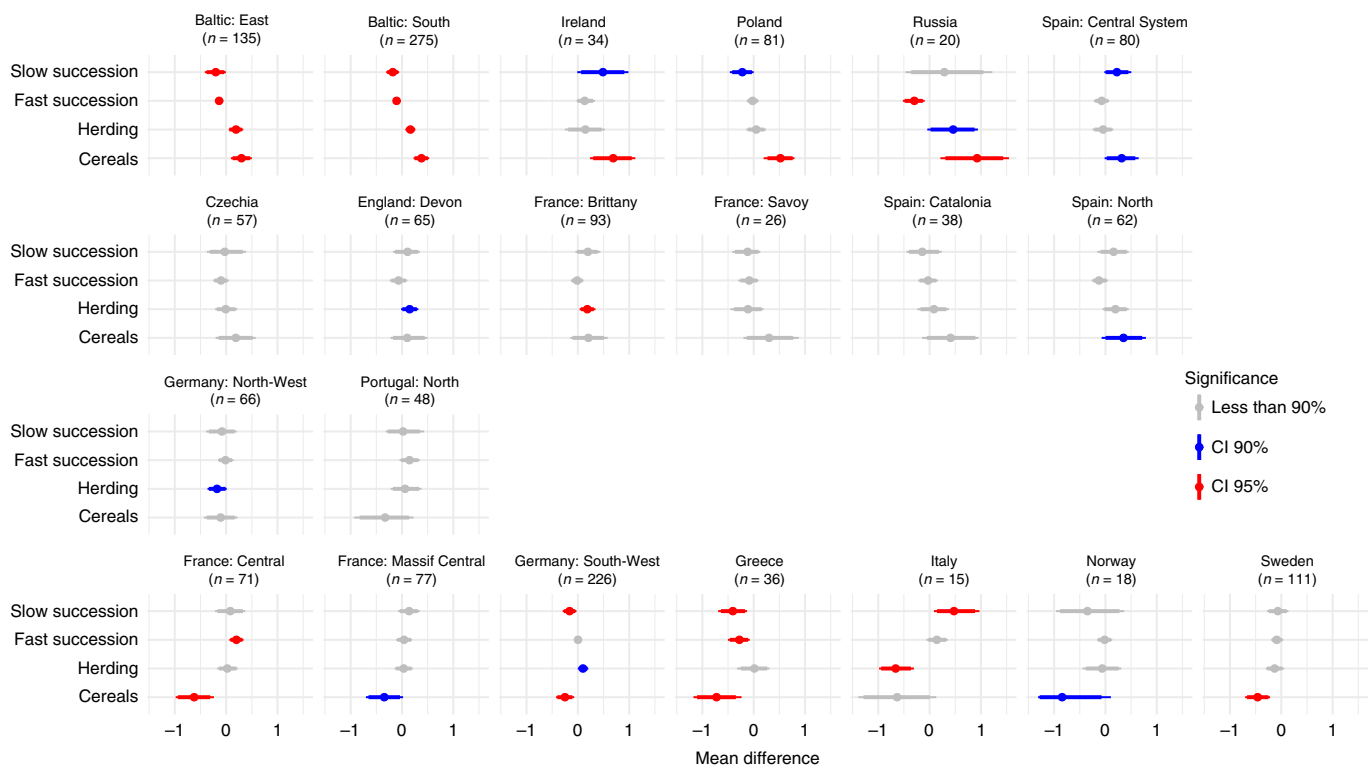


Fig. 4 | Regional-scale changes following Black Death in four BDP pollen indicators. Difference between the means of 100-yr periods of 1250–1350 CE and 1351–1450 CE, with the standard deviation. Statistical significance is based on bootstrap estimates. The indicators are presented in four rows from statistically significant increases in standardized mean percentages of cereal pollen (top) to statistically significant declines in standardized mean percentages of cereal pollen (bottom).

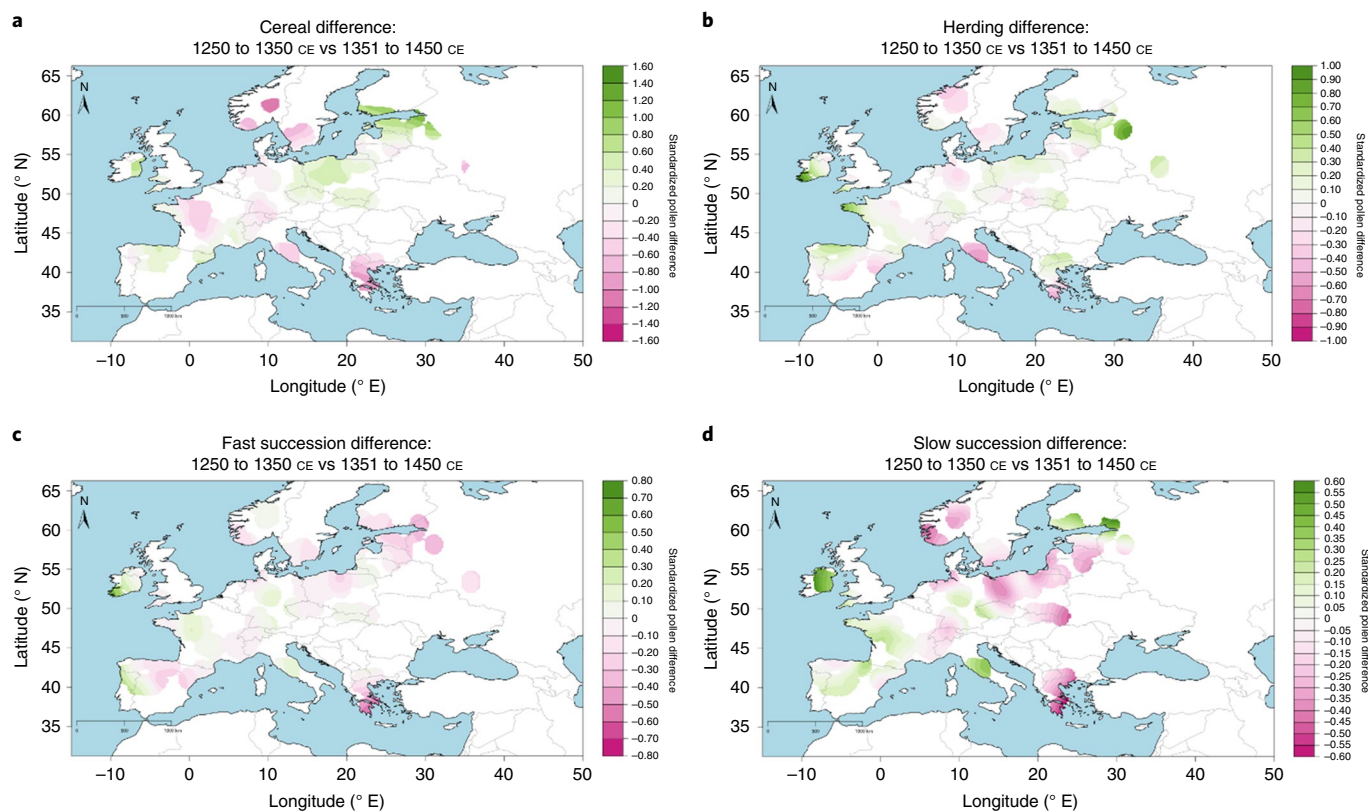


Fig. 5 | Spatial extrapolation showing 1250–1350 CE versus 1351–1450 CE temporal variation in the BDP pollen indicators. a–d, Cereal (a), herding (b), fast succession (c) and slow succession (d). Based on results from Supplementary Fig. 3.

largely uniform, strongly suggests that if early plague recurrences contributed considerably to the landscape change, the earliest of those recurrences, occurring within the first 25 years, were the most significant. Of course, if the *pestis secunda* partially accounts for the arable contraction and forest succession shown here for parts of Europe, our results would further call into question the demographic toll of the Black Death, even where we have discerned significant arable contraction, as in parts of France, Italy and Scandinavia. At the same time, if we are to include the earliest recurrences, where we have discerned little change or arable expansion, the significance of both the Black Death and those earliest recurrences is limited. These remarks aside, our approach has shown conclusively that the Black Death did not significantly alter land use everywhere or affect all regions equally. The significant variability in mortality that our BDP approach identifies remains to be explained, but local cultural, demographic, economic, environmental and societal contexts would have influenced *Y. pestis* prevalence, morbidity and mortality. Ongoing transformations of rural economy in many European regions would have also modified the plague mortality, or—to an extent—the amplified impact it had on the landscape. Importantly, regional population densities cannot explain the complex landscape dynamics we discern (as visualized in Supplementary Fig. 8), nor the geographical location of the 261 coring sites (see Supplementary Fig. 9, showing the averaged elevation of our sites). The spread of the pandemic depended on numerous factors, which would have generated compound effects, feedback loops and regionally unique outcomes. Plague is an ecologically and epidemiologically complex zoonotic disease, maintained by sylvatic rodents and their fleas, and transmittable to and between people via multiple pathways, including commensal and sylvatic rodent flea bites, respiratory secretions, direct contact with infected animals, human ectoparasites (fleas and lice) and fomites¹⁹. The behaviour of *Y. pestis* hosts and vectors, and

their capacity to efficiently transmit the pathogen, is partly constrained by complex interactions with seasonal climate variability and local ecological conditions, both in anthropogenic and rural environments (cities, villages and fields versus mountains, forests or wetlands³²). Regional variation in population density and distribution, ectoparasite burdens, living conditions, and commensal rodent populations and their fleas, undoubtedly mattered.

Local climatic contexts were also shown to have strongly determined third plague pandemic dynamics in Asia^{33,34}. In Europe, where the Black Death spread over several years (1347–1352 for the regions considered here), different seasons and annually variable climatic conditions may have influenced *Y. pestis* prevalence and the pandemic's mortality. Furthermore, while hypothesized links between early-fourteenth-century famines and the Black Death remain to be substantiated, and while *Y. pestis* is often lethal in lieu of antibiotics¹⁹, it has been shown that Black Death mortality was selective and the immunological and nutritional heterogeneity of the populations the pathogen interacted with would have ensured uneven toll^{35,36}.

That climatic, cultural, ecological and economic factors shaped regional Black Death outcomes is well illustrated by the initial phases of the pandemic in Europe. Cereal trade is thought to have been instrumental for the introduction of the pandemic to Mediterranean Europe, and along established conduits of commerce and communication, ecological factors, associated contingency effects and historical path dependency mattered from the outset. Before the pandemic arrived in the Crimea, the volume of cereal trade between Italy and the Black Sea was sizable, yet blocked by embargo^{11,37,38}. High demand in southern Europe for Black Sea cereals from 1345 onwards was associated with a period of excessive precipitation and cooling^{39,40} negatively affecting cereal supplies in Italy and beyond, 1345–47^{8,37,41,42}. Cereal imports from Black Sea

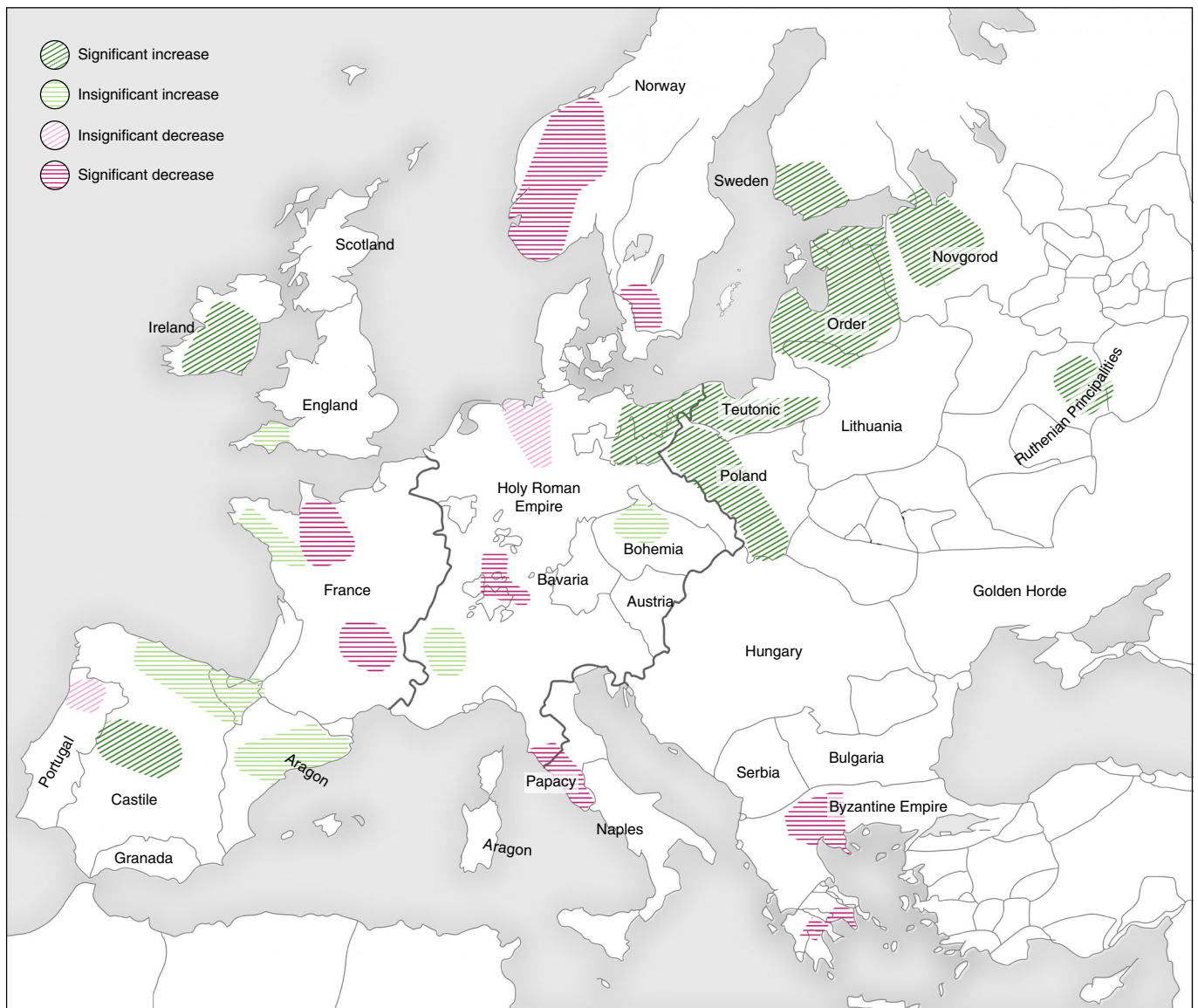


Fig. 6 | BDP-determined regional scenarios of Black Death demographic impact. Colours reflect centennial-scale changes in the cereal pollen indicators from Fig. 2. Background map with political borders of fourteenth-century Europe. Credit: Hans Sell, Michelle O'Reilly and A.I.

coasts resumed once the situation improved in 1347, and by early 1348 Venetian merchants had filled many Italian granaries with Black Sea produce^{11,37,39,43} and introduced plague to Europe. Plague outbreaks disseminated from major cereal ports in southern and north-western Italy from January 1348^{1,44}. To the contrary, plague hardly spread in north-western Italy, which was independent from overseas cereal imports^{37,43,45}. Local circumstances shaped the outcome of the pandemic on regional scales from the outset.

In summary, our BDP approach shows Black Death mortality was far more spatially heterogeneous than previously thought. This significant variation in Black Death mortality may be explained by the pathogen's entanglement with a dynamic nexus of cultural, ecological, economic, societal and climatic factors that determined its prevalence and the pandemic's mortality in any given region. That the pandemic was immensely destructive in some regions, but not all, falsifies the practice, not uncommon in Black Death studies, of predicting one region's experience on the basis of another's. Regional mortality outcomes must be reconstructed using local sources, including BDP as proxies of changes in cultural landscapes. As a few well-documented case studies of the Black Death's

destructive mortality in Europe have informed estimates of the pandemic's mortality not only in other European regions, but also in several regions of Africa and Asia, our findings have significant implications both for the wider history of the Black Death and for how historical disease outbreaks are reconstructed.

Methods

Pollen-inferred landscape change and pre-industrial demography. Recently, data derived from tree rings or ice cores have been employed to approximate changes in human economic activity related to past epidemics, as well as to warfare and climatic variability^{46,47}. However, none of these proxies is directly related to human demography or provides a basis to estimate variation in the Black Death's mortality on a regional scale across Europe (to date only a single archaeological study using pottery as a proxy for demographic change on the national level, focusing on just a single country—England—has appeared⁴⁸).

In recent years, pollen data have been proven to be closely related to demographic variability. Most importantly, detailed comparisons of historical documentary data on population trends and landscape changes as revealed by pollen data have been carried out on a local scale and a close link between changes in European pollen data and changes in European local demography over the past millennium has been demonstrated on multiple occasions, that is, during the period and region of our concern here^{49,50}. A strong link between long-term

demographic trends as visible in regional settlement numbers and macro-changes in land cover (deforestation/afforestation) have also been confirmed for ancient Greece³¹. Additionally, a recent publication successfully employed pollen data to test the extent of the mortality associated with the sixteenth-century Spanish and Portuguese empires' colonization of tropical regions in the Americas and Asia³². However, as of now there is no method to quantify past demographic trends in absolute numbers based on palaeoecological data. Consequently, we also focus in this paper on relative changes in historical societies' populations and test the now common idea that the Black Death caused enormous mortality across Europe (with many scholars now arguing for a mortality exceeding 30% and upwards of 50% of the population within a few years) (see also Fig. 1). Using our BDP approach, we conclude this hypothesis is not maintainable. Our evidence for demography-related landscape changes (or lack thereof) negates it.

Our main indicator is cereal pollen. In pre-industrial economies, rural labour availability (hence rural population levels) and the spatial scale of cereal cultivation were directly related. An increase in the extent and intensity of cereal cultivation—as reflected in pollen data—would have required not only a predilection and demand for cereals, but also greater availability of labour and thus population growth or significant immigration. The maintenance of existing agricultural activity, in turn, would have required relatively stable population levels^{33–35}. The uniform ~50% mortality postulated for the Black Death across Europe should have resulted in a large and significant decline of cereal cultivation and parallel forest regrowth across Europe, as previously demonstrated for mid-fourteenth-century Sweden²⁶ and singular sites in some regions of western Europe³⁶. This result agrees with the fact that Black Death mortality could be high among people at productive age, as illustrated for England^{37–38}. Moreover, even in the case of England, a comparatively commercialized and adaptive rural economy in mid-fourteenth-century Europe, the loss of 50% of the population led to a significant decline in the total area under cultivation (as documented by heterogeneous written sources)³⁹. In Italy, another well-developed economy at that time, the expansion of large estates following the Black Death also did not compensate for the general loss of cereal productivity⁴⁰. This effect, high mortality driving arable contraction, must have been yet more pronounced in more subsistence-oriented and less adaptive economies, with limited surplus production, such as in regions of the Iberian Peninsula, Germany, Sweden and particularly east-central Europe. Importantly, palaeoecological evidence for arable contraction may be indicative, to some extent, of not only rural population decline but also urban population decline in the region, as there is evidence in some areas, following the pandemic, of rural-to-urban migration, of country-dwellers repopulating urban centres⁴⁰. Possibly less common was intraregional rural migration, as marginal lands were abandoned for better quality soils, which were more likely to remain under cultivation^{26,61}.

Therefore, cereal pollen remains our most potent pollen indicator related to demographic changes in pre-industrial European societies. Other pollen indicators, reflecting rewilding and reforestation (secondary ecological succession) of cereal fields abandoned as a result of significant mortality, or the transformation of cereal fields into pastures, which required less rural labour and thus also could have been a response to high plague mortality, play a secondary role in our analysis and provide further support for our conclusions.

BDP data collection. Existing online palynological databases (the European Pollen Database (EPD)⁶² www.europeanpollendatabase.net, and the Czech Quaternary Palynological Database (PALYCZ)⁶³, <https://botany.natur.cuni.cz/palycz/>), as well as personal contacts of the study authors and a systematic publication search were employed to identify palynological sites in Europe reaching the required chronological and resolution quality for the study of the last millennium. In order to enable statistical analysis, we included only sites clustered in well-defined historical-geographical regions, excluding isolated sites even if the quality of a site's data was very good. Data of sufficient quality and amount from regions for which the Black Death is well-studied, notably central and northern England and the Low Countries, is not presently available; to the best of our knowledge, for each of these regions there currently is not more than a single isolated site³⁶, which does not allow for the application of statistical approaches.

In total, 261 pollen records with the average temporal resolution of 58 years and ¹⁴C-age control (or varve chronology), have been collected. The age–depth models of the sequences have been provided by authors in original publications, by the EPD or developed through the Clam package (version 2.3.4) of R software for the purpose of this study. The analytical protocol for pollen extraction and identification is reported in the original publications. The Pollen Sum includes all the terrestrial taxa with some exceptions based on the selection done in the original publications. The full list of sequences, exclusions from the Pollen Sum, age–depth models and full references are reported in Supplementary Data 1.

The taxa list has been normalized by applying the EPD nomenclature. In this respect, the general name Cichorioideae includes Asteraceae subf. Cichorioideae of the EPD and PALYCZ nomenclatures, which primarily refers to the fenestrate pollen of the Cichorieae tribe⁶⁴. Ericaceae groups *Arbutus unedo*, *Calluna vulgaris*, *Vaccinium* and different *Erica* pollen types, whereas deciduous *Quercus* comprehends both *Q. robur* and *Q. cerris* pollen types⁶⁵. Rosaceae refers to both tree and herb species of the family. Finally, *Rumex* includes *R. acetosa*

type, *R. acetosella*, *R. crispus* type, *Rumex/Oxyria* and *Urtica* groups *U. dioica* type and *U. pilulifera*.

BDP summary pollen indicators. In order to connect changes visible in the pollen data to human demographic trajectories, we assembled four summary pollen indicators that describe specific landscapes related to human activity. They reflect different degrees of demographic pressure on the landscape (cereal cultivation, pastoral activities, which are less-labour intensive than cereal cultivation, abandonment and rewilding) as well as different durations of land abandonment that might have occurred post-Black Death. Our indicators account for the fact that Europe is a continent rich in natural heritage, with a wide range of landscapes and habitats and a remarkable wealth of flora and fauna, shaped by climate, geomorphology and human activity. In order to ensure uniform interpretation of the indicators, we relied on criteria that can be applied to all European landscapes regardless of their local specificity. Cereals and herding are directly related to human activities and are barely influenced by spatial differences. More complex is the succession of natural plants with their ecological behaviour and inter-species competition. For this reason, we relied on existing quantitative indicators of plant ecology.

The Ellenberg L – light availability indicator⁶⁶ provides a measure of sunlight availability in woodlands and consequently of tree-canopy thickness, reflecting the scale of the natural regeneration of woodland vegetation after cultivation or pasture activities⁶¹. Nonetheless, ecological studies have suggested that geographic and climatic variability between different European regions can influence the Ellenberg indicator system^{67–71}. The original indicators were primarily designed for Central Europe⁶⁸, but several studies developed Ellenberg indicators for other regions, reflecting the specific ecology of the selected taxa (British Isles;⁷² Czech Republic;⁷³ Greece;⁷⁴ Italy;⁷⁵ Sweden⁷⁶). Plants with L values between 5 and 8 are listed in the fast succession indicator, the ones with L values ranging from 1 to 4 are included in the slow succession indicator. The result is the following list:

1) **Cereals:** only cultivated cereals have been included: *Avena/Triticum* type, Cerealia type, *Hordeum* type, *Secale*. 2) **Herding** includes pastoral indicators linked to the redistribution of human pressure: *Artemisia*, Cichorioideae, *Plantago lanceolata* type, *Plantago major/media* type, *Polygonum aviculare* type, *Rumex*, *Trifolium* type, *Urtica*, *Vicia* type. 3) **Fast Succession** comprises indicators of relatively recent reforestation of cultivated land after abandonment: *Alnus*, *Betula*, *Corylus*, Ericaceae, *Fraxinus ornus*, *Juniperus*, *Picea*, *Pinus*, *Populus*, deciduous *Quercus*, Rosaceae. 4) **Slow Succession** includes indicators of secondary succession established after several decades of abandonment: *Abies*, *Carpinus betulus*, *Fagus*, *Fraxinus*, *Ostrya/Carpinus orientalis*, *Quercus ilex* type.

In order to validate the indicators overcoming the regional limits of Ellenberg values, a different subdivision has been provided following the Niinemets and Valladares shade tolerance scale for woody species of the Northern Hemisphere⁷⁷. The subdivision of taxa in the Fast and Slow succession indicators remains the same with only three changes: *Fraxinus ornus* and *Picea* move from Fast to Slow succession and *Fraxinus* from Slow to Fast succession. Extended Data Figs. 1 and 2 show that the two groupings yield the same results, which confirms the reliability of our indicators. There is only one clear exception (Russia), with one more region where smaller-scale diversion occurs for only one indicator, Slow Succession (Norway). The different indicator behaviour results from the different attribution of *Picea* in our two sets of succession indicators: at high latitude, *Picea* characterizes the final stage of the ecological succession and hence its different attribution results in different summary indicator values in Russia for the two stages of ecological succession, fast and slow.

Please note our summary indicators are not designed to reflect the entirety of the landscape and reconstruct all of its different components. Rather, they are a means of approximating changes in the landscape related to the types of human activities, and their intensity, as much as they relate to demographic changes in human populations using and inhabiting these landscapes.

BDP analytical statistical and spatial methods. To control for local specificity, pollen percentages of every taxon from each pollen site were standardized. From the taxa percentage in a given year the arithmetic mean calculated for the observations from the period 1250–1450 was subtracted and the result divided by the standard deviation for the 1250–1450 period. Standardized taxa results were assembled for each site into four BDP summary indicators. Since each indicator has different numbers of taxa, the sum of standardized taxa values calculated for a given year and site was divided by the number of taxa in the indicator. For the purposes of replication, this standardized pollen dataset, comprising the four indicators for each sample from each site, is available as Supplementary Data 2.

This dataset has been analysed in two ways, statistically and spatially.

For the statistical approach, standardized regional indices of landscape transformation were created for each region by calculating the average value for all sites within the region, for each of the subperiods analysed in the study (1250–1350 and 1351–1450; 1301–1350 and 1351–1400; 1325–1350 and 1351–1375). Differences between means for each subperiod were measured by the use of the bootstrapping based on 10,000 resamples. The 90% and 95% confidence intervals were estimated with the bias-corrected and accelerated method (BCa)⁷⁸. These results are visualized in Fig. 5 for the comparison of the subperiods of 1250–1350

versus 1351–1450, and in Supplementary Figs. 4 and 6 for the comparison of the subperiods of 1300–1350 versus 1351–1400 and 1325–1350 versus 1351–1375, respectively.

For the spatial approach, we employed the Bayesian model AverageR developed within the Pandora and IsoMemo initiatives (<https://pandoraapp.earth/>) to map the distribution of pollen indices across Europe. AverageR is a generalized additive model that has been described previously⁷⁹. It relies on a thin-plate regression spline⁸⁰ to predict new, unseen data using the following model:

$$Y_i = g(\text{longitude}, \text{latitude}) + \varepsilon_i$$

Where Y_i is the independent variable for site i ; $g(\text{longitude}, \text{latitude})$ is the spline smoother; and $\varepsilon_i \sim N(0, \sigma\varepsilon)$ is the error term.

The spline smoother can be written as $X \times \beta$ where X is a fixed design matrix and β is the parameter vector. Surface smoothing is controlled by employing a Bayesian smoothing parameter estimated from the data and trades-off bias against variance to make the optimal prediction⁷⁵. This parameter β is assumed to follow a normal distribution: $\beta \sim N(0, 1/\delta \times \lambda \times P)$, where P is a so-called penalty matrix of the thin plate regression spline, which penalizes second derivatives⁸¹. The δ parameter is by default set to 1 but this can be adjusted to suit smoothing needs for each application. In our study δ was set at 0.9 to match the preferred spatial scale of analysis for our dataset (approx. 250 to 500 km).

AverageR was employed to generate smoothed surfaces for three sets of temporal bins (1250–1350 versus 1351–1450, as well as 1300–1350 versus 1351–1400 and 1325–1350 versus 1351–1375) and for the four BDP indicators (Supplementary Figs. 3, 5 and 7). For the same indicator the difference between the two temporal bins was plotted (Fig. 5; Supplementary Figs. 4 and 6).

Reporting Summary. Further information on research design is available in the Nature Research Reporting Summary linked to this article.

Data availability

All data generated or analysed during this study are included in this published article (as the Supplementary Data).

Received: 30 June 2021; Accepted: 15 December 2021;

Published online: 10 February 2022

References

- Benedictow, O. L. *The Black Death 1346–1353: The Complete History* (Boydell, 2004).
- Mohammed, M. *Peste, Contagion et Martyre: Histoire du Fléau en Occident Médiéval* (Publisud, 2005).
- Varlik, N. *Plague and Empire in the Early Modern Mediterranean World: the Ottoman Experience, 1347–1600* (Cambridge Univ. Press, 2015).
- Aberth, J. *The Black Death: A New History of the Great Mortality in Europe, 1347–1500* (Oxford Univ. Press, 2021).
- Bos, K. I. et al. A draft genome of *Yersinia pestis* from victims of the Black Death. *Nature* **478**, 506–510 (2011).
- Spyrou, M. A. et al. Phylogeography of the second plague pandemic revealed through analysis of historical *Yersinia pestis* genomes. *Nat. Commun.* **10**, 4470 (2019).
- Herlihy, D. Climate and documentary sources: a comment. *J. Interdiscip. Hist.* **10**, 713–717 (1980).
- Campbell, B. *The Great Transition: Climate, Disease and Society in the Late-Medieval World* (Cambridge Univ. Press, 2016).
- Chouin, G. L. Reflections on plague in African history (14th–19th c.). *Afriques* **9**, 2228 (2018).
- Roosen, J. & Curtis, D. R. Dangers of noncritical use of historical plague data. *Emerg. Infect. Dis.* **24**, 103–110 (2018).
- Barker, H. Laying the corpses to rest: grain, embargoes, and *Yersinia pestis* in the Black Sea, 1346–48. *Speculum* **96**, 97–126 (2020).
- Green, M. The four black deaths. *Am. Historical Rev.* **125**, 1601–1631 (2020).
- Hecker, J. *Der Schwarze Tod* (1832).
- Hatcher, J. *Plague, Population, and the English Economy, 1348–1530* (Macmillan, 1977).
- Ormrod, W. M. & Lindley, P. G. *The Black Death in England, 1348–1500* (Paul Watkins, 1996).
- Roosen, J. & Curtis, D. R. The 'light touch' of the Black Death in the Southern Netherlands: an urban trick? *Economic Hist. Rev.* **72**, 32–56 (2019).
- Wray, S. K. *Communities and Crisis. Bologna During the Black Death* (Brill, 2009).
- Biraben, J. N. *Les Hommes et la Peste en France et Dans les Pays Européens et Méditerranéens* (Mouton, 1975).
- Dubyanskiy, V. M. & Yeszhanov, A. B. *Ecology of Yersinia pestis and the Epidemiology of Plague. In Yersinia pestis: Retrospective and Perspective* (eds. Yang, R. & Anisimov, A.) 101–170 (Springer Netherlands, 2016).
- Christakos, G. *Interdisciplinary Public Health Reasoning and Epidemic Modelling: The Case of Black Death* (Springer, 2005).
- Olea, R. A. & Christakos, G. Duration of urban mortality for the 14th-century Black Death epidemic. *Hum. Biol.* **77**, 291–303 (2005).
- Alfani, G. Plague in seventeenth-century Europe and the decline of Italy: an epidemiological hypothesis. *Eur. Rev. Economic Hist.* **17**, 408–430 (2013).
- Neithard, B. in *Histoire des Populations de l'Europe* (eds. Dupâquier, J. & Bardet, J.-P.) 168–184 (Fayard, 1997).
- Echenberg, M. *Plague Ports: The Global Urban Impact of Bubonic Plague, 1894–1901* (NYU Press, 2007).
- Tumbe, C. *Pandemics and Historical Mortality in India* (IIMA, 2020).
- Lagerås, P. et al. in *Environment, Society and the Black Death: An Interdisciplinary Approach to the Late-Medieval Crisis in Sweden* (ed. Lagerås, P.) 30–68 (Oxbow Books, 2016).
- Małowist, M. *Western Europe, Eastern Europe and World Development, 13th–18th centuries: Collection of Essays of Marian Małowist* (Brill, 2010).
- Guzowski, P., Kuklo, C. & Poniat, R. in *Epidemie w dziejach Europy: konsekwencje społeczne, gospodarcze i kulturowe* (eds. Polek, K. & Sroka, E. T.) 119–144 (Wydawnictwo Naukowe Uniwersytetu Pedagogicznego, 2016).
- Myrdal, J. in *When Disease Makes History: Epidemics and Great Historical Turning Points* (ed. Hämmäläinen, P.) 141–186 (Helsinki Univ. Press, 2006).
- Myrdal, J. in *Living with the Black Death* (eds. Bisgaard, L. & Sondergaard, L.) 63–84 (Univ. Press of Southern Denmark, 2011).
- Poos, L. *Rural Society after the Black Death* (Cambridge Univ. Press, 2011).
- Slavin, P. Out of the West: formation of a permanent plague reservoir in South-Central Germany (1349–1356) and its implications. *Past Present* **252**, 3–51 (2021).
- Xu, L. et al. Nonlinear effect of climate on plague during the third pandemic in China. *Proc. Natl Acad. Sci. USA* **108**, 10214–10219 (2011).
- Xu, L. et al. Wet climate and transportation routes accelerate spread of human plague. *Proc. Biol. Sci.* **281**, 20133159 (2014).
- DeWitte, S. Stature and frailty during the Black Death: the effect of stature on risks of epidemic mortality in London, A.D. 1348–1350. *J. Arch. Sci.* **39**, 1412–1419 (2012).
- Crespo, F. & Lawrenz, M. B. Heterogeneous immunological landscapes and medieval plague: an invitation to a new dialogue between historians and immunologists. *Medieval Globe* **1**, 229–258 (2014).
- Pinto, G. Firenze e la carestia del 1346–47: Aspetti e problemi delle crisi annonarie alla metà del '300. *Archivio Stor. Ital.* **130**, 3–84 (1972).
- Faugeron, F. *Nourrir la ville: ravitaillement, marchés et métiers de l'alimentation à Venise dans les derniers siècles du Moyen Âge* (2014).
- Luterbacher, J. et al. European summer temperatures since Roman times. *Environ. Res. Lett.* **11**, 024001 (2016).
- Esper, J. et al. Eastern Mediterranean summer temperatures since 730 CE from Mt. Smolikas tree-ring densities. *Clim. Dyn.* **54**, 1367–1382 (2020).
- Campbell, B. *The European Mortality Crises of 1346–52 and Advent of the Little Ice Age. In Famines During the 'Little Ice Age' (1300–1800) Socionatural Entanglements in Premodern Societies 19–41* (Springer, 2017).
- Bauch, M. & Engel, A. *Die 1340er Jahre als Schlüsseljahrzehnt der 'Great Transition': Eine klimahistorische Perspektive auf den Vorabend des Schwarzen Todes. In Pest! Sonderausstellung des LWL-Museums für Archäologie - Westfälisches Landesmuseum Herne* (eds. Berner, A., Leenen, S. & Maus, S.) 76–82 (WBG, 2019).
- Hübner, H.-J. *Quia bonum sit anticipare tempus. Die kommunale Versorgung Venedigs mit Brot und Getreide vom späten 12. bis ins 15. Jahrhundert* (Lang, 1998).
- Del Panta, L. *Le epidemie nella storia demografica italiana. (secoli XIV–XIX)* (Loescher, 1980).
- Santorio, C. *Gli uffici del Comune di Milano e del Dominio visconteo-sforzesco <1216–1515>* (Giuffrè, 1968).
- Ljungqvist, F. C. et al. Linking European building activity with plague history. *J. Archaeol. Sci.* **98**, 81–92 (2018).
- McConnell, J. R. et al. Pervasive Arctic lead pollution suggests substantial growth in medieval silver production modulated by plague, climate, and conflict. *Proc. Natl Acad. Sci. USA* **116**, 14910–14915 (2019).
- Lewis, C. Disaster recovery: new archaeological evidence for the long-term impact of the 'calamitous' fourteenth century. *Antiquity* **90**, 777–797 (2016).
- Lamentowicz, M. et al. How Joannites' economy eradicated primeval forest and created anthroecosystems in medieval Central Europe. *Sci. Rep.* **10**, 18775 (2020).
- Czerwiński, S. et al. Environmental implications of past socioeconomic events in Greater Poland during the last 1200 years. Synthesis of paleoecological and historical data. *Quat. Sci. Rev.* **259**, 106902 (2021).
- Izdebski, A., Słoczyński, T., Bonnier, A., Koloch, G. & Kouli, K. Landscape change and trade in ancient Greece: evidence from pollen data. *Economic J.* **130**, 2596–2618 (2020).
- Hamilton, R. et al. Non-uniform tropical forest responses to the 'Columbian Exchange' in the Neotropics and Asia-Pacific. *Nat. Ecol. Evol.* **5**, 1174–1184 (2021).

53. Izdebski, A. *A Rural Economy in Transition: Asia Minor from Late Antiquity into the Early Middle Ages* (Taubenschlag Foundation, 2013).
54. Roberts, N. et al. Europe's lost forests: a pollen-based synthesis for the last 11,000 years. *Sci. Rep.* **8**, 716 (2018).
55. Bevan, A. et al. The changing face of the Mediterranean – Land cover, demography and environmental change: Introduction and overview. *Holocene* **29**, 703–707 (2019).
56. Yeloff, D. & Van Geel, B. Abandonment of farmland and vegetation succession following the Eurasian plague pandemic of ad 1347–52. *J. Biogeogr.* **34**, 575–582 (2007).
57. Razi, Z. *Life, Marriage, and Death in a Medieval Parish: Economy, Society, and Demography in Halesowen, 1270–1400* (University Press, 1980).
58. DeWitte, S. N. Age patterns of mortality during the Black Death in London, A.D. 1349–1350. *J. Archaeol. Sci.* **37**, 3394–3400 (2010).
59. Broadberry, S. N. *British Economic Growth, 1270–1870* (University Press, 2015).
60. Cortonesi, A. in *Medioevo delle campagne: rapporti di lavoro, politica agraria, protesta contadina* (eds. Cortonesi, A. & Piccinni, G.) 15–56 (Viella, 2011).
61. Abel, W. *Agrarkrisen und Agrarkonjunktur. Eine Geschichte der Land- und Ernährungswirtschaft Mitteleuropas seit dem hohen Mittelalter* (Parey, 1978).
62. Fyfe, R. et al. The European Pollen Database: past efforts and current activities. *Vegetation Hist. Archaeobotany* **18**, 417–424 (2009).
63. Kuneš, P., Abraham, V., Kovářík, O. & Kopecký, M. Czech Quaternary Palynological Database – PALYCZ: review and basic statistics of the data. *Preslia* **81**, 209–238 (2009).
64. Florenzano, A., Marignani, M., Rosati, L., Fascetti, S. & Mercuri, A. M. Are Cichorieae an indicator of open habitats and pastoralism in current and past vegetation studies? *Plant Biosyst.* **149**, 154–165 (2015).
65. Smit, A. A scanning electron microscopic study of the pollen morphology in the genus *Quercus*. *Acta Botanica Neerlandica* **22**, 655–665 (1973).
66. Ellenberg, H. et al. Zeigerwerte von Pflanzen in Mitteleuropa. *Scr. Geobotanica* **18**, 1–258 (1992).
67. Dzwonko, Z. Assessment of light and soil conditions in ancient and recent woodlands by Ellenberg indicator values. *J. Appl. Ecol.* **38**, 942–951 (2001).
68. Diekmann, M. & Lawesson, J. E. Shifts in ecological behaviour of herbaceous forest species along a transect from northern central to North Europe. *Folia Geobotanica* **34**, 127–141 (1999).
69. Gégout, J.-C. & Krizova, E. Comparison of indicator values of forest understory plant species in Western Carpathians (Slovakia) and Vosges Mountains (France). *For. Ecol. Manag.* **182**, 1–11 (2003).
70. Hájková, P., Hájek, M., Apostolova, I., Zelený, D. & Dítě, D. Shifts in the ecological behaviour of plant species between two distant regions: evidence from the base richness gradient in mires. *J. Biogeogr.* **35**, 282–294 (2008).
71. Wasof, S. et al. Ecological niche shifts of understorey plants along a latitudinal gradient of temperate forests in north-western Europe. *Glob. Ecol. Biogeogr.* **22**, 1130–1140 (2013).
72. Hill, M., Mountford, J., Roy, D. & Bunce, R. *Ellenberg's indicator Values for British Plants* Vol. 2 Technical Annex. (Institute of Terrestrial Ecology, 1999).
73. Chytrý, M., Tichý, L., Dřevojan, P., Sádlo, J. & Zelený, D. Ellenberg-type indicator values for the Czech flora. *Preslia* **90**, 83–103 (2018).
74. Böhlting, N., Greuter, W. & Raus, T. Zeigerwerte der Gefäßpflanzen der Südägäis (Griechenland). Indicator values of the vascular plants in the Southern Aegean (Greece). *Braun-Blanquetia* **32**, 1–106 (2002).
75. Pignatti, S., Menegoni, P. & Pietrosanti, S. Biondificazione attraverso le piante vascolari. Valori di indicazione secondo Ellenberg (Zeigerwerte) per le specie della Flora d'Italia. *Braun-Blanquetia* **39**, 1–97 (2005).
76. Diekmann, M. Use and improvement of Ellenberg's indicator values in deciduous forests of the Boreo-nemoral zone in Sweden. *Ecography* **18**, 178–189 (1995).
77. Niinemets, Ü. & Valladares, F. Tolerance to shade, drought, and waterlogging of temperate Northern Hemisphere trees and shrubs. *Ecol. Monogr.* **76**, 521–547 (2006).
78. Hall, P. Theoretical comparison of bootstrap confidence intervals. *Ann. Stat.* **16**, 927–953 (1988).
79. Cubas, M. et al. Latitudinal gradient in dairy production with the introduction of farming in Atlantic Europe. *Nat. Commun.* **11**, 2036 (2020).
80. Wood, S. N. Thin plate regression splines. *J. R. Stat. Soc. Ser. B* **65**, 95–114 (2003).
81. Groß, M. Modeling body height in prehistory using a spatio-temporal Bayesian errors-in variables model. *Adv. Stat. Anal.* **100**, 289–311 (2016).

Acknowledgements

The authors acknowledge the following funding sources: Max Planck Independent Research Group, Palaeo-Science and History Group (A.I., A.M. and C.V.); Estonian Research Council #PRG323, PUT1173 (A.Pos., T.R., N.S. and S.V.); European Research Council #FP7 263735 (A.Bro. and A.Plu.), #MSC 655659 (A.E.); Georgetown Environmental Initiative (T.N.); Latvian Council of Science #LZP-2020/2-0060 (N.S. and N.J.); LLNL-JRNL-820941 (I.T.); NSF award #GSS-1228126 (S.M.); Polish-Swiss Research Programme #013/2010 CLIMPEAT (M.Lam.), #086/2010 CLIMPOL (A.W.); Polish Ministry of Science and Higher Education #N N306 275635 (M.K.); Polish National Science Centre #2019/03/X/ST10/00849 (M.Lam.), #2015/17/B/ST10/01656 (M.Lam.), #2015/17/B/ST10/03430 (M.Slo.), #2018/31/B/ST10/02498 (M.Slo.), #N N304 319636 (A.W.); SCIEX #12.286 (K.Mar.); Spanish Ministry of Economy and Competitiveness #REDISCO-HAR2017-88035-P (J.A.L.S.); Spanish Ministry of Education, Culture and Sports #FPU16/00676 (R.L.L.); Swedish Research Council #421-2010-1570 (P.L.), #2018-01272 (F.C.L. and A.S.); Volkswagen Foundation Freigeist Fellowship Dantean Anomaly (M.B.); Spanish Ministry of Science and Innovation #RTI2018-101714-B-I00 (F.A.S. and D.A.S.), OP RDE, MEYS project #CZ.02.1.01/0.0/0.0/16_019/0000728 (P.P.).

Author contributions

A.I., A.M. and P.G. designed the study. A.I. drafted the paper with contributions from M.B., R.Fer., G.P., A.M., T.N., P.G., R.P., F.C.L. and C.V.; A.M., L.M., J.P. and C.V. created the pollen database, with the support of J.A.L.S. (Spain), P.L. (Sweden) and T.R. (Estonia). A.I., R.P., R.Fer. and C.C. carried out the analyses. A.S., D.A.S., F.A.S., L.B., A.Bra., A.Bro., S.C., A.E., M.F., A.F., E.D.F., R.Fyf., N.J., P.K., K.K., R.K., M.K., M.Lam., M.Lin., R.L.L., K.Mar., F.M., S.M., A.M.M., K.Mil., Y.M., A.M.N., E.N., M.O., S.P., M.L.P., A.Ped., S.P.D., G.P., A.Plu., P.P., A.Pos., M.R., L.S., C.S.F., D.S., M.Slo., M.Sta., N.S., I.T., S.V. and A.W. provided palynological data and contributed to the text and the interpretation.

Funding

Open access funding provided by Max Planck Society.

Competing interests

The authors declare no competing interests.

Additional information

Extended data is available for this paper at <https://doi.org/10.1038/s41559-021-01652-4>.

Supplementary information The online version contains supplementary material available at <https://doi.org/10.1038/s41559-021-01652-4>.

Correspondence and requests for materials should be addressed to A. Masi.

Peer review information *Nature Ecology & Evolution* thanks José Sebastián Carrión García and the other, anonymous, reviewer(s) for their contribution to the peer review of this work. Peer reviewer reports are available.

Reprints and permissions information is available at www.nature.com/reprints.

Publisher's note Springer Nature remains neutral with regard to jurisdictional claims in published maps and institutional affiliations.

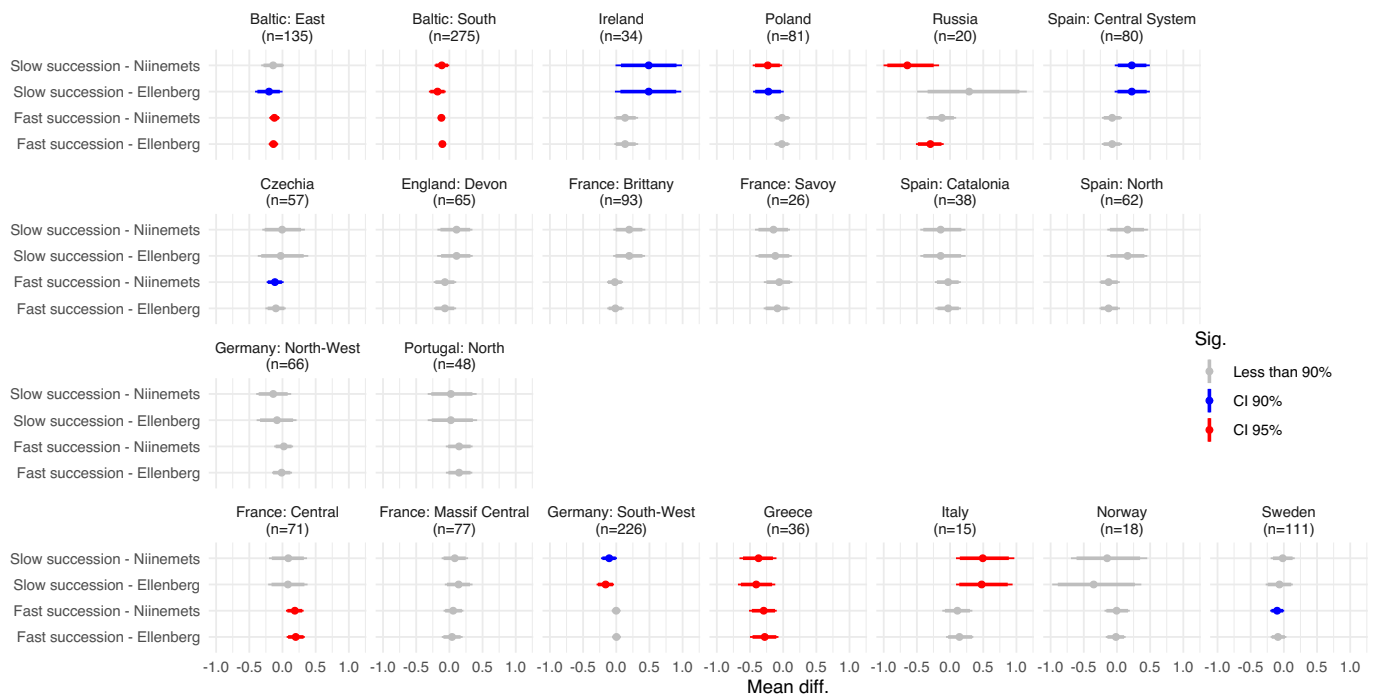


Open Access This article is licensed under a Creative Commons Attribution 4.0 International License, which permits use, sharing, adaptation, distribution and reproduction in any medium or format, as long as you give appropriate credit to the original author(s) and the source, provide a link to the Creative Commons license, and indicate if changes were made. The images or other third party material in this article are included in the article's Creative Commons license, unless indicated otherwise in a credit line to the material. If material is not included in the article's Creative Commons license and your intended use is not permitted by statutory regulation or exceeds the permitted use, you will need to obtain permission directly from the copyright holder. To view a copy of this license, visit <http://creativecommons.org/licenses/by/4.0/>.

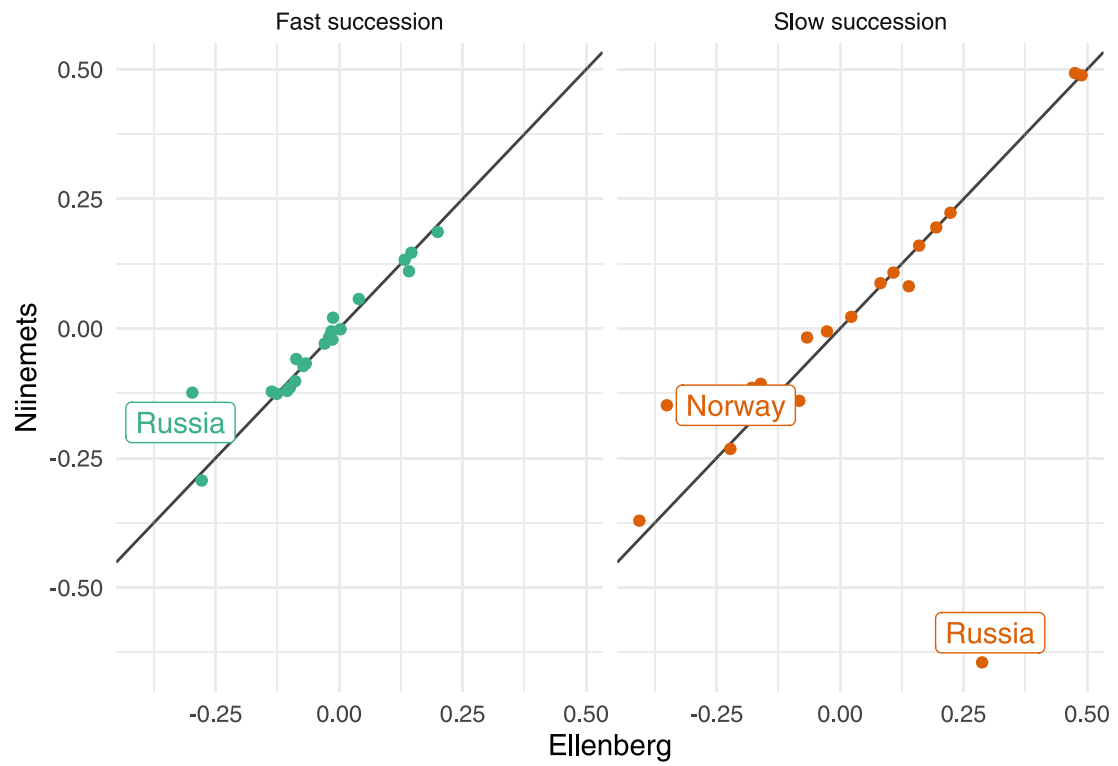
© The Author(s) 2022

¹Max Planck Institute for the Science of Human History, Jena, Germany. ²Institute of History, Jagiellonian University in Krakow, Krakow, Poland. ³Faculty of History and International Relations, University of Białystok, Białystok, Poland. ⁴Department of Earth Science, Sapienza University of Rome, Rome, Italy. ⁵Department of Environmental Biology, Sapienza University of Rome, Rome, Italy. ⁶Department of Agriculture and Forest Sciences (Dafne), University of Tuscia, Viterbo, Italy. ⁷Department of Ecological and Biological Sciences (Deb), University of Tuscia, Viterbo, Italy. ⁸Leibniz Institute for the History and Culture of Eastern Europe (GWZO), Leipzig, Germany. ⁹ArchaeoBioCenter, Ludwig-Maximilians-Universität München, München, Germany. ¹⁰School of Archaeology, University of Oxford, Oxford, UK. ¹¹Faculty of Arts, Masaryk University, Brno, Czech Republic. ¹²Department of History, Stockholm University, Stockholm, Sweden. ¹³Bolin Centre for Climate Research, Stockholm University, Stockholm, Sweden. ¹⁴Swedish Collegium for Advanced Study, Uppsala, Sweden. ¹⁵Department of History, Georgetown University, Washington DC, USA. ¹⁶Department of Biology, Georgetown University, Washington DC,

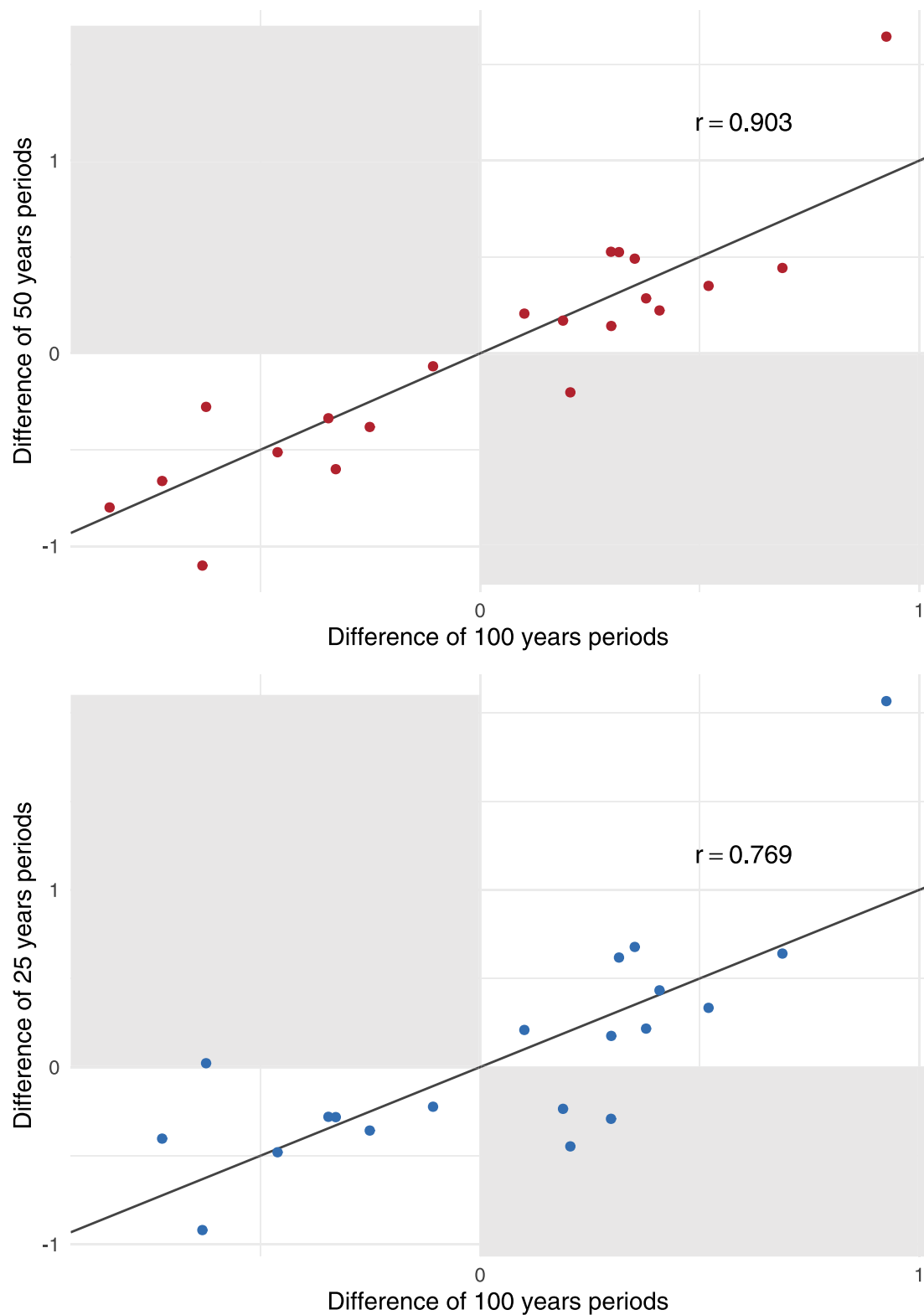
USA. ¹⁷Chair of Forest Growth and Dendroecology, Institute of Forest Sciences, Albert-Ludwigs-University Freiburg, Freiburg, Germany. ¹⁸Department of Botany, University of Innsbruck, Innsbruck, Austria. ¹⁹Department of Botany, University of Granada, Granada, Spain. ²⁰Viscum Pollenanalys & Miljöhistoria, Nässjö, Sweden. ²¹GFZ-German Research Centre for Geosciences, Section Climate Dynamics and Landscape Evolution, Potsdam, Germany. ²²Institute of Geosciences, University of Potsdam, Potsdam, Germany. ²³Wessex Archaeology, Portway House, Salisbury, UK. ²⁴Department of Archaeology, University of Reading, Reading, UK. ²⁵Climate Change Ecology Research Unit, Adam Mickiewicz University, Poznań, Poland. ²⁶CNRS, Université Clermont Auvergne, GEOLAB, Clermont-Ferrand, France. ²⁷ISEM, UMR 5554, Université Montpellier, CNRS, EPHE, IRD, Montpellier, France. ²⁸Department of Palaeobiology, Faculty of Biology, University of Białystok, Białystok, Poland. ²⁹Laboratory of Palynology and Palaeobotany, Department of Life Sciences, University of Modena and Reggio Emilia, Modena, Italy. ³⁰Museum of Archaeology, University of Stavanger, Stavanger, Norway. ³¹School of Geography, Earth and Environmental Science, University of Plymouth, Plymouth, UK. ³²Department of Geography, University of Latvia, Riga, Latvia. ³³Department of Geology and Geoenvironment, National and Kapodistrian University of Athens, Athens, Greece. ³⁴Institute of Archeology, Academy of Sciences of the Czech Republic, Prague, Czech Republic. ³⁵The Archaeologists, National Historical Museums, Lund, Sweden. ³⁶Southern Swedish Forest Research Centre, Swedish University of Agricultural Sciences, Alnarp, Sweden. ³⁷Environmental Archaeology Research Group, Institute of History, CSIC, Madrid, Spain. ³⁸Department of Geography, Universidad Autónoma de Madrid, Madrid, Spain. ³⁹Department of Environmental Geography, GEODE UMR 5602, Jean Jaurès University, Toulouse, France. ⁴⁰Department of Geography, University of Nevada, Reno, USA. ⁴¹Anthropocene Research Unit, Faculty of Geographical and Geological Sciences, Adam Mickiewicz University, Poznań, Poland. ⁴²CNRS, HNHP UMR 7194, Muséum National d'Histoire Naturelle, Institut de Paléontologie Humaine, Paris, France. ⁴³Institute of Archaeology, Faculty of History, Nicolaus Copernicus University, Toruń, Poland. ⁴⁴Centre for Climate Change Research, Nicolaus Copernicus University, Toruń, Poland. ⁴⁵Faculty of Geography, Lomonosov Moscow State University, Moscow, Russia. ⁴⁶Department of Quaternary Research, Institute of Geography Russian Academy of Science, Moscow, Russia. ⁴⁷Institute of Geological Sciences, Polish Academy of Sciences, Warsaw, Poland. ⁴⁸Laboratory of Forest Botany-Geobotany, School of Forestry and Natural Environment, Aristotle University of Thessaloniki, Thessaloniki, Greece. ⁴⁹Institute of Geography, University of Cologne, Cologne, Germany. ⁵⁰Laboratory of Palaeoecology and Archaeobotany, Department of Plant Ecology, Faculty of Biology, University of Gdańsk, Gdańsk, Poland. ⁵¹Department of Geography, Urban and Regional Planning, Universidad de Cantabria, Santander, Spain. ⁵²Centre for Theoretical Study, Charles University and Academy of Sciences of the Czech Republic, Prague, Czech Republic. ⁵³Department of Geology, Tallinn University of Technology, Tallinn, Estonia. ⁵⁴Department of Physical Geography and Ecosystem Science, Lund University, Lund, Sweden. ⁵⁵Institute of Ecology and Earth Sciences, University of Tartu, Tartu, Estonia. ⁵⁶Department of Pre- and Early History and West Asian Archaeology, University of Heidelberg, Heidelberg, Germany. ⁵⁷School of Natural and Built Environment, Queen's University, Belfast, Northern Ireland. ⁵⁸IFP Energies Nouvelles, Earth Sciences and Environmental Technologies Division, Rueil-Malmaison, Rueil-Malmaison, France. ⁵⁹Past Landscape Dynamics Laboratory, Institute of Geography and Spatial Organization, Polish Academy of Sciences, Warsaw, Poland. ⁶⁰Nature Research Centre, Institute of Geology and Geography, Vilnius, Lithuania. ⁶¹Institute of Latvian History, University of Latvia, Riga, Latvia. ⁶²Center for Accelerator Mass Spectrometry (CAMS), Lawrence Livermore National Laboratory, Lawrence, CA, USA. ⁶³W. Szafer Institute of Botany, Polish Academy of Sciences, Kraków, Poland. [✉]e-mail: alessia.masi@uniroma1.it



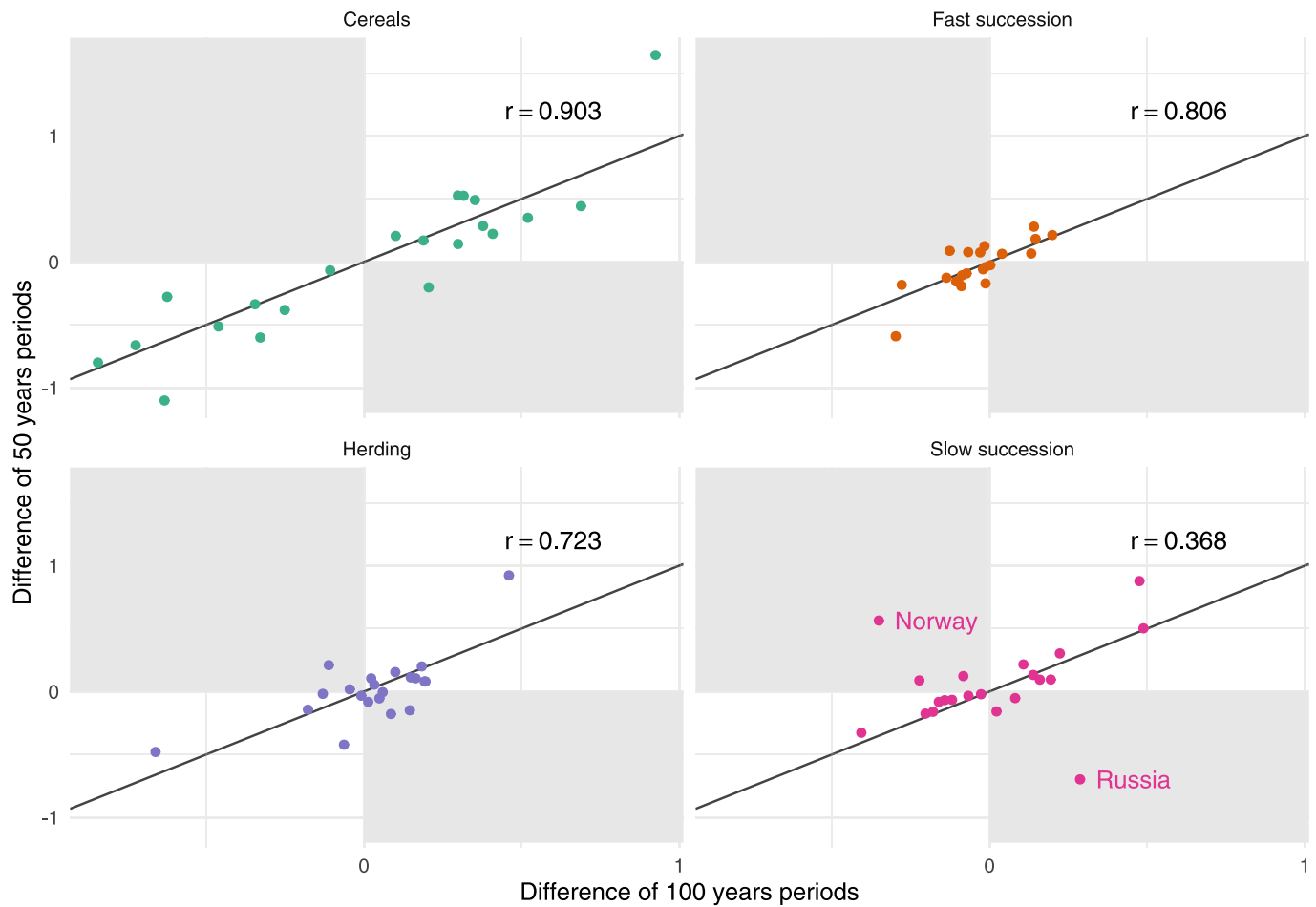
Extended Data Fig. 1 | Region-by-region comparison of Ellenberg and Niinemets indicators.



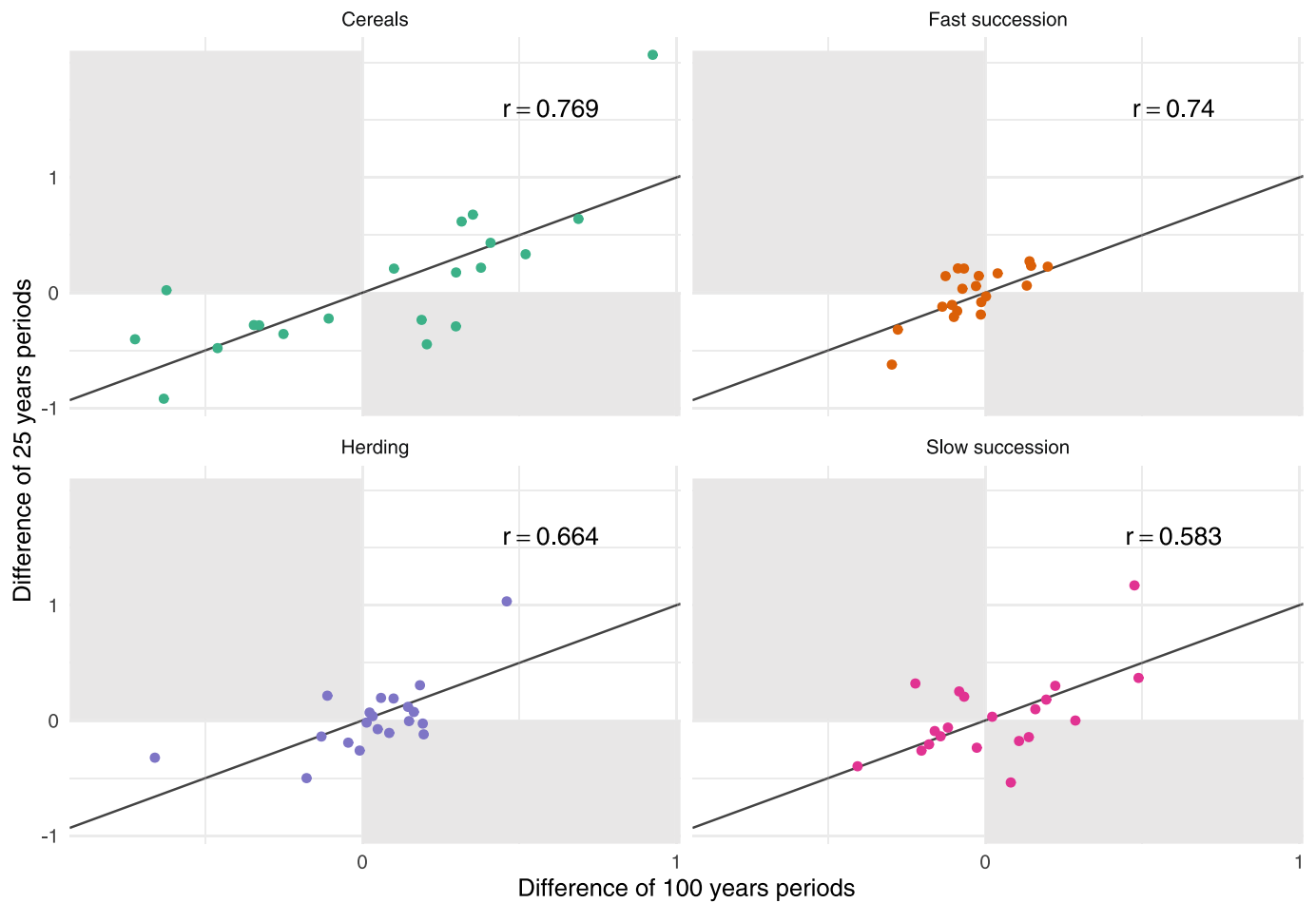
Extended Data Fig. 2 | Outlier analysis of Ellenberg and Niinemets indicators.



Extended Data Fig. 3 | Differences and similarities in the changes in the cereal pollen indicator between 100-yr periods of analysis versus 50-yr and 25-yr periods respectively. Points displayed in white areas represent regions where the direction of changes was the same over the longer versus shorter periods of time. Points displayed in grey areas represent regions where the direction of changes was different over the longer versus shorter periods of time. Regions showing such differences have been named. Based on Supplementary Figs. 1 and 2.



Extended Data Fig. 4 | Differences and similarities in the changes in the BDP pollen indicators between 100-yr and 50-yr periods of analysis. Points displayed in white areas represent regions where the direction of changes was the same over the longer versus shorter periods of time. Points displayed in grey areas represent regions where the direction of changes was different over the longer versus shorter periods of time. Based on Supplementary Fig. 1. Please note: Norway and Russia were the only regions that showed significant differences between Ellenberg and Niinemets indicators, most strongly for the slow succession indicator. Based on Supplementary Fig. 1.



Extended Data Fig. 5 | Differences and similarities in the changes in the BDP pollen indicators between 100-yr and 25-yr periods of analysis. Points displayed in white areas represent regions where the direction of changes was the same over the longer versus shorter periods of time. Points displayed in grey areas represent regions where the direction of changes was different over the longer versus shorter periods of time. Based on Supplementary Fig. 2.

Reporting Summary

Nature Portfolio wishes to improve the reproducibility of the work that we publish. This form provides structure for consistency and transparency in reporting. For further information on Nature Portfolio policies, see our [Editorial Policies](#) and the [Editorial Policy Checklist](#).

Statistics

For all statistical analyses, confirm that the following items are present in the figure legend, table legend, main text, or Methods section.

n/a Confirmed

- The exact sample size (n) for each experimental group/condition, given as a discrete number and unit of measurement
- A statement on whether measurements were taken from distinct samples or whether the same sample was measured repeatedly
- The statistical test(s) used AND whether they are one- or two-sided
Only common tests should be described solely by name; describe more complex techniques in the Methods section.
- A description of all covariates tested
- A description of any assumptions or corrections, such as tests of normality and adjustment for multiple comparisons
- A full description of the statistical parameters including central tendency (e.g. means) or other basic estimates (e.g. regression coefficient) AND variation (e.g. standard deviation) or associated estimates of uncertainty (e.g. confidence intervals)
- For null hypothesis testing, the test statistic (e.g. F , t , r) with confidence intervals, effect sizes, degrees of freedom and P value noted
Give P values as exact values whenever suitable.
- For Bayesian analysis, information on the choice of priors and Markov chain Monte Carlo settings
- For hierarchical and complex designs, identification of the appropriate level for tests and full reporting of outcomes
- Estimates of effect sizes (e.g. Cohen's d , Pearson's r), indicating how they were calculated

Our web collection on [statistics for biologists](#) contains articles on many of the points above.

Software and code

Policy information about [availability of computer code](#)

Data collection

Data analysis

For manuscripts utilizing custom algorithms or software that are central to the research but not yet described in published literature, software must be made available to editors and reviewers. We strongly encourage code deposition in a community repository (e.g. GitHub). See the Nature Portfolio [guidelines for submitting code & software](#) for further information.

Data

Policy information about [availability of data](#)

All manuscripts must include a [data availability statement](#). This statement should provide the following information, where applicable:

- Accession codes, unique identifiers, or web links for publicly available datasets
- A description of any restrictions on data availability
- For clinical datasets or third party data, please ensure that the statement adheres to our [policy](#)

Field-specific reporting

Please select the one below that is the best fit for your research. If you are not sure, read the appropriate sections before making your selection.

Life sciences Behavioural & social sciences Ecological, evolutionary & environmental sciences

For a reference copy of the document with all sections, see [nature.com/documents/nr-reporting-summary-flat.pdf](https://www.nature.com/documents/nr-reporting-summary-flat.pdf)

Ecological, evolutionary & environmental sciences study design

All studies must disclose on these points even when the disclosure is negative.

Study description	The regional variation in the Black Death's impact in Europe has been investigated using a new approach, Big Data Palaeoecology (BDP), based on collecting and analyzing existing pollen sequences from 19 European countries (published as well as unpublished).
Research sample	In order to create our dataset, we used existing online palynological databases (the European Pollen Database, www.europeanpollendatabase.net , and the Czech Quaternary Palynological Database, https://botany.natur.cuni.cz/palycz/), as well as personal contacts of the study authors and a systematic publication search. In this way, we identified palynological sites in Europe that meet the necessary chronological and resolution quality criteria for the investigated period of time (1250-1450 CE).
Sampling strategy	Pollen sequence with sufficient resolution (average temporal resolution of 58 years) and 14C-age control (or varve chronology) have been selected and grouped according to regional clusters. Single isolated sites from outside these clusters have been excluded because they do not allow the application of quantitative analysis.
Data collection	Pollen percentages of selected taxa have been collected from the 261 pollen sequences included in the study.
Timing and spatial scale	Europe, 1250-1450 CE
Data exclusions	Pollen sequences with low resolution; no cereal pollen; insufficient chronological control; no accompanying sites in the same region.
Reproducibility	The analytical protocol for pollen extraction and identification is reported in the original publications. The Pollen Sum includes all the terrestrial taxa with some exceptions based on the selection done in the original publications. The full list of sequences, exclusions from the Pollen Sum, age-depth models and full references are reported in Supplementary Data 1.
Randomization	The sequences are grouped in regions according to spatial distribution
Blinding	n/a
Did the study involve field work?	<input type="checkbox"/> Yes <input checked="" type="checkbox"/> No

Reporting for specific materials, systems and methods

We require information from authors about some types of materials, experimental systems and methods used in many studies. Here, indicate whether each material, system or method listed is relevant to your study. If you are not sure if a list item applies to your research, read the appropriate section before selecting a response.

Materials & experimental systems

n/a	Involved in the study
<input checked="" type="checkbox"/>	<input type="checkbox"/> Antibodies
<input checked="" type="checkbox"/>	<input type="checkbox"/> Eukaryotic cell lines
<input checked="" type="checkbox"/>	<input type="checkbox"/> Palaeontology and archaeology
<input checked="" type="checkbox"/>	<input type="checkbox"/> Animals and other organisms
<input checked="" type="checkbox"/>	<input type="checkbox"/> Human research participants
<input checked="" type="checkbox"/>	<input type="checkbox"/> Clinical data
<input checked="" type="checkbox"/>	<input type="checkbox"/> Dual use research of concern

Methods

n/a	Involved in the study
<input checked="" type="checkbox"/>	<input type="checkbox"/> ChIP-seq
<input checked="" type="checkbox"/>	<input type="checkbox"/> Flow cytometry
<input checked="" type="checkbox"/>	<input type="checkbox"/> MRI-based neuroimaging